frontiers | Frontiers in Molecular Neuroscience

TYPE Original Research
PUBLISHED 29 April 2024
DOI 10.3389/fnmol.2024.1356544

OPEN ACCESS

EDITED BY
Katsuhiko Tabuchi,
Shinshu University, Japan

REVIEWED BY
James Y. H. Li,
University of Connecticut Health Center, United States
G. Giacomo Consalez,
Vita-Salute San Raffaele University, Italy

*CORRESPONDENCE
Daniel Goldowitz
dang@cmmt.ubc.ca

RECEIVED 15 December 2023
ACCEPTED 12 April 2024
PUBLISHED 29 April 2024

CITATION
Gupta I, Yeung J, Rahimi-Balaei M, Wu S-R and Goldowitz D (2024) Msx genes delineate a novel molecular map of the developing cerebellar neuroepithelium.
Front. Mol. Neurosci. 17:1356544.
doi: 10.3389/fnmol.2024.1356544

Msx genes delineate a novel molecular map of the developing cerebellar neuroepithelium

Ishita Gupta[1,2], Joanna Yeung[1,2], Maryam Rahimi-Balaei[1,2], Sih-Rong Wu[3] and Dan Goldowitz[1,2]*

[1]British Columbia Children's Hospital, Vancouver, BC, Canada, [2]Department of Medical Genetics, University of British Columbia, Vancouver, BC, Canada, [3]Department of Neuroscience, Baylor College of Medicine, Houston, TX, United States

In the early cerebellar primordium, there are two progenitor zones, the ventricular zone (VZ) residing atop the IVth ventricle and the rhombic lip (RL) at the lateral edges of the developing cerebellum. These zones give rise to the several cell types that form the GABAergic and glutamatergic populations of the adult cerebellum, respectively. Recently, an understanding of the molecular compartmentation of these zones has emerged. To add to this knowledge base, we report on the *Msx* genes, a family of three transcription factors, that are expressed downstream of Bone Morphogenetic Protein (BMP) signaling in these zones. Using fluorescent RNA *in situ* hybridization, we have characterized the *Msx* (Msh Homeobox) genes and demonstrated that their spatiotemporal pattern segregates specific regions within the progenitor zones. *Msx1* and *Msx2* are compartmentalized within the rhombic lip (RL), while *Msx3* is localized within the ventricular zone (VZ). The relationship of the *Msx* genes with an early marker of the glutamatergic lineage, *Atoh1*, was examined in *Atoh1*-null mice and it was found that the expression of *Msx* genes persisted. Importantly, the spatial expression of *Msx1* and *Msx3* altered in response to the elimination of *Atoh1*. These results point to the Msx genes as novel early markers of cerebellar progenitor zones and more importantly to an updated view of the molecular parcellation of the RL with respect to the canonical marker of the RL, *Atoh1*.

KEYWORDS

cerebellar development, BMP signaling, mouse, atoh1, MSX genes

Introduction

During early embryonic development, the neuroepithelium of the cerebellar primordium consists of two primary progenitor zones – the rhombic lip (RL) and the ventricular zone (VZ). The evidence indicates that all glutamatergic cells (glutamatergic cerebellar nuclear neurons, granule cells and unipolar brush cells) arise from the RL while the GABAergic cells (GABAergic cerebellar nuclear neurons, Purkinje cells and interneurons) arise from the VZ (Hoshino et al., 2005; Machold and Fishell, 2005; Wang et al., 2005; Supplementary Figure S1). The two progenitor zones are molecularly defined by the non-overlapping expressions of two basic Helix–Loop–Helix (bHLH) transcription factors–*Atoh1* (formerly termed *Math1*) for the RL (Machold and Fishell, 2005; Wang et al., 2005) and *Ptf1a* for the VZ (Hoshino et al., 2005). Since these progenitor zones give rise to several cell types over time, it would be important to identify the molecular pathways within the RL and the VZ that play roles in the determination of the different cell types that are generated in the neuroepithelia.

BMP signaling has been studied in cerebellar development and has been shown to be necessary for normal development of both glutamatergic and GABAergic lineages (Alder et al., 1999; Qin et al., 2006; Tong and Kwan, 2013; Ma et al., 2020). Activated R-smad is expressed in both the RL and the VZ (Fernandes et al., 2012; Tong and Kwan, 2013). Studies have shown that loss of both BMP signaling components, Smad1 and Smad5 (R-smads), in cerebellum results in defects in RL stem cell specification, loss of nuclear transitory zone (NTZ) and reduced external germinal layer (EGL); and activation of the BMP antagonist NBL1 suppresses RL cell specification (Krizhanovsky and Ben-Arie, 2006; Tong and Kwan, 2013). Overexpressing Smad7 (I-smad that inhibits BMP signaling) in the midbrain-hindbrain boundary (MHB) via *Wnt1*-Cre leads to loss of the choroid plexus and cerebellar morphologic anomalies (Tang et al., 2010). Smad7 is expressed in the EGL suggesting that activated BMP signaling is not required or suppressed in later development processes like EGL formation (Lai et al., 2011). Involvement of BMP signaling in the VZ lineages has had more limited exploration. While the loss of *Smad4* (Co-smad) does not affect the glutamatergic lineage, *En1*-Cre knock-out of *Smad4* results in reduced number of Purkinje cells (Zhou et al., 2003). At an earlier age of E11.5, conditional knock-out of *Smad4* using *En1*-Cre significantly reduces the proliferative KI67-positive VZ progenitors (Fernandes et al., 2012). Recently, a study by Ma et al. (2020) has shown that the gradual spatiotemporal decline in the BMP/Smad gradient across the dorso-ventral axis of the VZ directs the identity transition of the VZ progenitor cells from Olig2-positive Purkinje neuron progenitors to Gsx1-positive interneuron progenitors (Ma et al., 2020). While it is clear that BMP signaling is important to the developing cerebellum, it is not clear what are the downstream genetic and transcriptional changes that mediate this signaling in the cerebellum, particularly in the progenitor zones of the RL and VZ.

The *Msx* (Msh Homeobox) genes are directly activated by BMP signaling in mice and are suitable candidates for mediating BMP signaling in cerebellar development (Suzuki et al., 1997; Takahashi et al., 1998). These homeobox-containing genes are known transcriptional repressors (Catron et al., 1995, 1996; Zhang et al., 1996; Newberry et al., 1997). The mouse family consists of three members - Msx1, Msx2 and Msx3. These 3 genes share 98% sequence similarity in their homeodomains (Ekker et al., 1997). Mouse Msx3 and the putative human ortholog VENTX (based on NCBI's Eukaryotic Genome Annotation pipeline) do not share sequence homology, hinting at species-based differences in functions and redundancy of the Msx family. In mice, Msx1 and Msx2 have been extensively studied in the context of craniofacial morphogenesis and limb organogenesis (Satokata and Maas, 1994; Foerst-Potts and Sadler, 1997; Satokata et al., 2000; Wu et al., 2003); while in neural development they are known to be expressed in overlapping patterns in many regions including roof plate cells and the adjacent neural tube (Tríbulo et al., 2003; Sunkin et al., 2013; Duval et al., 2014). Msx3 has been relatively less studied in the context of development although it is exclusively expressed only in the dorsal CNS in mice, particularly the developing spinal cord and the cerebellum (Wang et al., 1996; Sunkin et al., 2013). Based on the expression of the *Msx* genes in the E9.5-E10.5 murine neural tube, along with strong expression in the neural plate of cephalochordates (Sharman et al., 1999) and ascidians (Ma et al., 1996), this family of genes seems to have a strong conserved function in dorsal neural tube patterning.

We found that all 3 *Msx* genes are expressed early in our cerebellar time-course FANTOM5 transcriptome dataset (Arner et al., 2015; Ha et al., 2019). From the perspective of an importance of BMP signaling in the early developing cerebellum, and that the Msx genes could be mediators of this signaling with the early specific expression in the cerebellum, we sought to explore possible roles of this family of genes in the context of mouse cerebellar development.

Results

Msx genes are expressed only in the progenitor zones at early time-points

As a first step toward understanding the temporal expression patterns of the *Msx* transcription factors (TFs), we examined the FANTOM5 time-course transcriptome for the developing cerebellum (Ha et al., 2019). All three Msx TFs have a highly dynamic temporal expression signature, with a steep decline after E11.5-E12.5 (Figures 1A–C). The peak times of *Msx1* and *Msx3* expression are at the early embryonic stages. *Msx2* has a biphasic expression pattern, showing expression at the early embryonic time and an early postnatal expression.

To evaluate spatial expression of the *Msx* genes, we used chromogenic RNA *in situ* hybridization (ISH) to probe for the mRNA on sagittal sections of the developing cerebellum (see Methods for probe and tissue details). *Msx1* is expressed in the rhombic lip (RL) at both E11.5 and E12.5 (white arrows in Figures 1D,G). During the same time, *Msx3* expression is restricted to the ventricular zone (VZ) (black arrows in Figures 1E,H). With this *in situ* method, Msx2 expression is found throughout the neuroepithelia, but the boundaries of its expression are less clear (Figures 1F,I). Expressions of *Msx1* and *Msx3* get more restricted with finer defined boundaries at E12.5 compared to E11.5. At E12.5 across the medio-lateral axis, Msx1 and Msx2 expressing domains do not show any variation; on the other hand, the dorsal end of Msx3 expressing domain in the VZ is closer to the RL region in more medial positions. Thus, at these early ages, the expressions of all the *Msx* genes are concentrated in the progenitor zones of the neuroepithelium and are absent from the rest of the cerebellar primordium.

Msx1 and Msx2 expressing cells are compartmentalized within the rhombic lip at E12.5

As indicated in the Introduction, *Msx1* and *Msx2* have been shown to have overlapping expression domains outside of the cerebellum, with sometimes similar and/or redundant functions. Our chromogenic ISH demonstrated that both *Msx1* and *Msx2* are expressed in the cerebellar RL. To further examine their relationship in the cerebellar RL, RNAscope fluorescent *in situ* hybridization (FISH) multiplex assay (Wang et al., 2012) was used to double-label *Msx1* and *Msx2* mRNAs. Expression of *Msx1* and *Msx2* was also compared to the *Atoh1* expression, which molecularly delineates the ventral boundary of the RL (yellow dotted line in Figure 2) and distinguishes the RL from the VZ (Wang et al., 2005). Of interest, both *Msx1* and *Msx2* are expressed in cells within the RL but they are expressed in different populations of

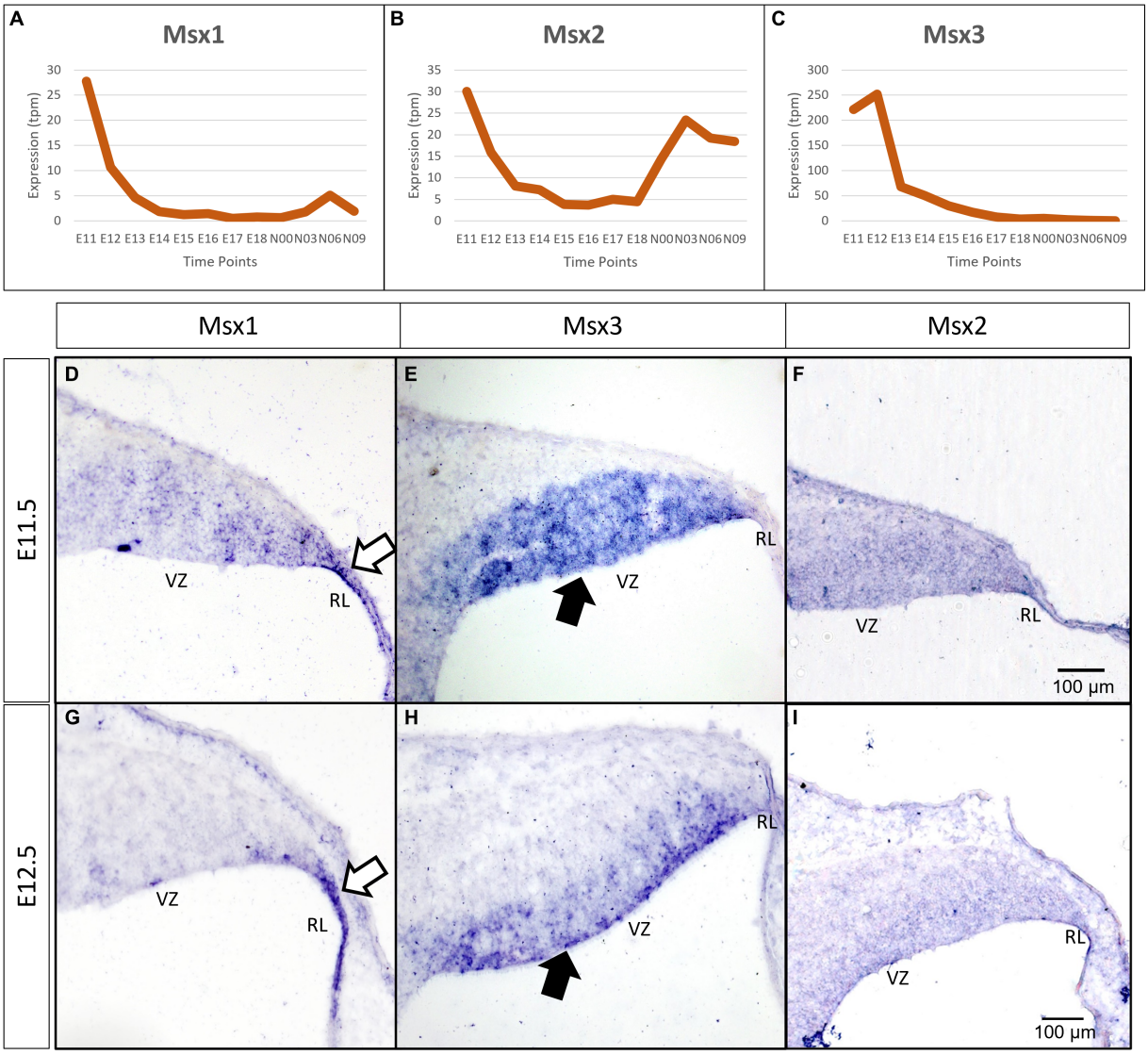

FIGURE 1
Temporal and spatial expression of Msx genes in the developing cerebellum. **(A–C)** Graphs show the dynamic nature of Msx expression in the cerebellum across 12 developmental time-points as observed from the RIKEN FANTOM5 transcriptome time-course data. **(D–I)** Sagittal sections of the RL with the right-side of panels denoting posterior and the bottom-side denoting ventral, with RNA *in situ* hybridization showing Msx genes expressed in the progenitor zones in **(D–F)** E11.5 and **(G–I)** E12.5. Msx1 expression is limited to the RL (white arrows in **D**,**G**) whereas Msx3 is limited to the VZ (black arrows in **E**,**H**). Msx2 expression is detected in the neuroepithelium but the boundary of the expression is not clear **(F,I)**. See supplementary Figure S2 for negative control staining. RL, Rhombic Lip; VZ, Ventricular Zone. Scale bar, 100 µm.

cells (Figure 2A). At E12.5 *Msx1* is expressed most strongly in the posterior-most tip of the RL that is *Atoh1* negative (white arrows in Figures 2A,B,D) with much weaker expression in the rest of the RL. This is also observed at E11.5 (Supplementary Figure S4). The same observation of non-overlapping Msx1 and Atoh1 expression at E12.5 is reproduced using antibodies targeting Msx1 and Atoh1 with immunofluorescence (Figures 2H–J). *Msx2* expression is within the *Atoh1* expression domain and is not expressed in the *Atoh1*-negative *Msx1*-positive compartment (Figures 2A,C). Thus, *Msx1* and *Msx2* expression regions are non-overlapping and form an *Msx1-Msx2-Msx1* banding pattern (Figure 2A). At postnatal ages, *Msx2*, and not *Msx1*, expression is detected in the granule cells (Supplementary Figures S5C,D). A schematic illustration of this compartmentation at E12.5 is shown in Figure 2G.

The localization of Msx1 to the RL region posterior to the Atoh1-positive domain prompted us to further determine if Msx1 is expressed in another early determinant of the cerebellum, the roof plate. To this end, we examined the double labeling of Msx1 and Lmx1a, a known cell marker of rhombic lip and the roof plate (Casoni et al., 2020), with immunofluorescence (IF). At E12.5, Msx1-positive cells co-expressed Lmx1a, indicating that Msx1 is expressed in the cells of both the rhombic lip and the roof plate (Supplementary Figure S5).

Later at E14.5, chromogenic RNA *in situ* hybridization reveals that *Msx1* expression is most obvious in the iRL (interior RL) compartment (Figure 2K), a region defined by high Wls expression and low Atoh1 expression (Yeung et al., 2014). Immunofluorescent double labeling with Msx1 and Atoh1 antibodies detected Msx1 expression in the iRL

10.3389/fnmol.2024.1356544

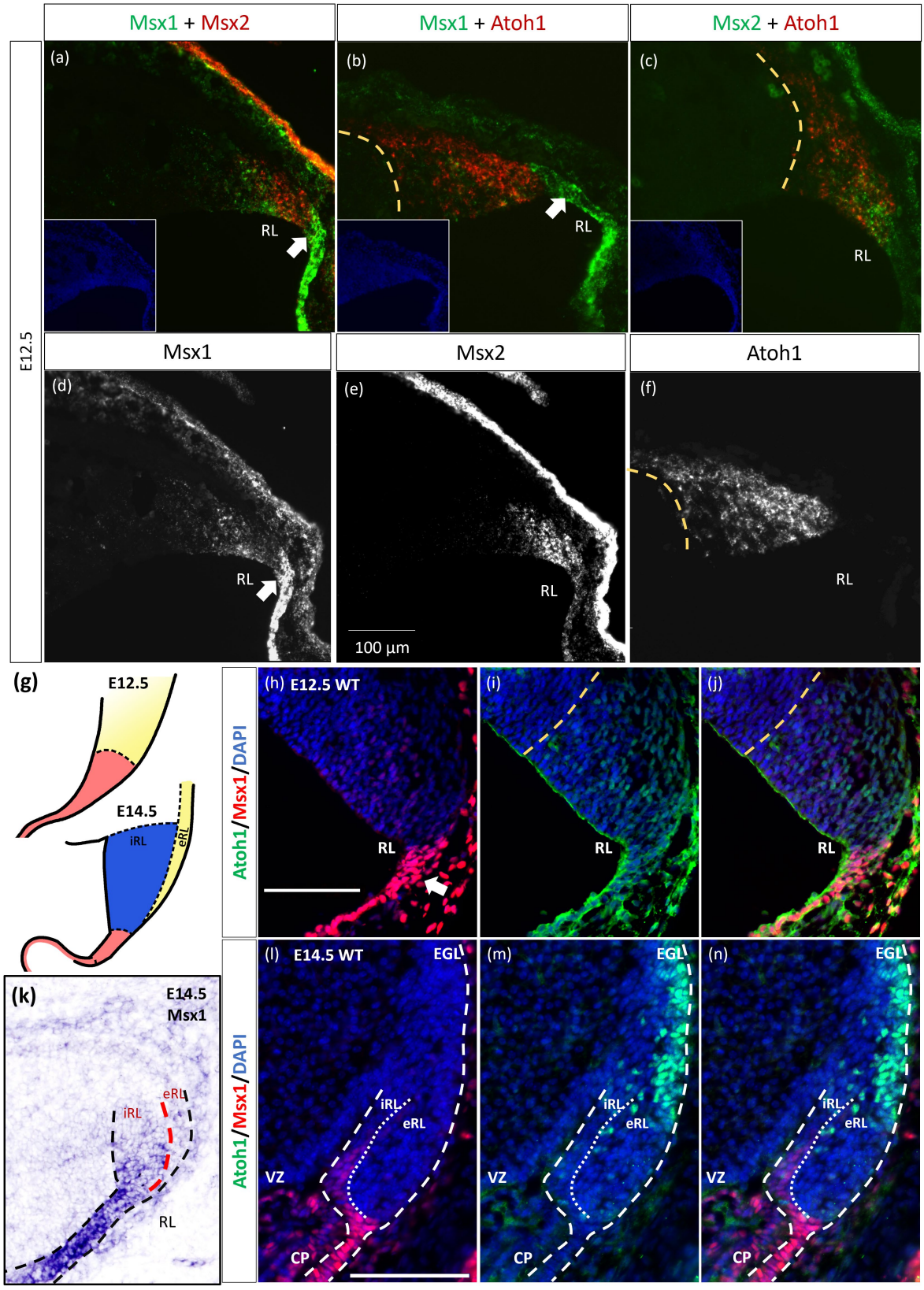

FIGURE 2
Msx1 and Msx2 expression relative to Atoh1 in the early cerebellum. **(A–F,H–N)** Sagittal sections of the RL with the right-side of panels denoting dorsal and the bottom-side denoting caudal. **(A–C)** RNAscope fluorescent RNA *in situ* hybridization (FISH) double-label on sagittal sections of E12.5 cerebellum. Dotted yellow lines **(A–J)** highlight the ventral boundary of RL as delineated by Atoh1 expression. **(A)** Msx1 (green) and Msx2 (red) expression regions form an alternative banding pattern and do not overlap with each other. Msx1 (green) is expressed highest in the distal tip of the RL

(Continued)

FIGURE 2 (Continued)
(white arrow) dorsal to Atoh1 (red). This compartment is Atoh1-negative **(B)** and maps to the red region shown in **(G)** at E12.5. **(C)** Msx2 (green) and Atoh1 (red) are largely overlapping in their expression regions. **(A-C)** Inset shows DAPI (blue) counterstain of the respective cerebellar tissue sections. Roof plate epithelium auto-fluoresces with the fluorescent dyes. **(D–F)** show the expression of Msx1, Msx2 and Atoh1, respectively. **(G)** Schematic illustrating the compartments within the RL at E12.5 and E14.5 based on results by Yeung et al. (2014). At both ages, red represents Wls-positive, Msx1-positive and Atoh1-negative, yellow represents Atoh1-positive, Wls-negative, Msx1-negative. At E14.5 the blue iRL region is Wls-positive and Atoh1-negative. **(H–J,L–N)** Immunofluorescence double-label on E12.5 and E14.5 cerebellum. At E12.5, **(H)** Msx1 (red) is expressed strongest in the caudal-most tip of the RL (white arrows) that is Atoh1 (green) negative **(I)**. **(J)** Merged Msx1 and Atoh1 staining at E12.5. **(K)** Chromogenic RNA *in situ* hybridization of Msx1 on sagittal E14.5 section shows stronger expression in the Wls-positive iRL than the eRL. At E14.5, Msx1 expression (red in l) is restricted to the interior face of the RL (iRL), that is negative for Atoh1 (green in m). **(N)** Merged Msx1 and Atoh1 staining illustrated the restricted expression for both molecules at E14.5. Refer to Appendix Figure 2 and 3 for negative control staining. CP, choroid plexus; EGL, external germinal layer; eRL, exterior RL; iRL, interior RL; RL, Rhombic Lip; VZ, ventricular zone. Scale bars, 100 μm.

(Figures 2L,N) but no expression of Atoh1 (Figure 2N). At this age Atoh1 expression is restricted to the eRL (exterior RL in Figures 2M,N); the two proteins do not overlap in the RL at E14.5. A schematic of this compartmentation at E14.5 is illustrated in Figure 2G.

The observation that Msx1 expression is highly restricted in the E14.5 iRL prompted us to examine its relationship with Wls, a known marker of the iRL (Yeung et al., 2014). To this end, we examined Msx1 expression in the *Wls*-reporter mouse strain that expresses βgal under the *Wls* promoter at both E12.5 and E14.5 (Yeung et al., 2014). Double labeling of Msx1 and βgal in E12.5 *Wls*-reporter cerebellum demonstrated an overlapping expression of both molecules in cells at the tip of the RL and the rest of the RL area (red arrows in Figure 3). Msx1 expression, however, is absent in the stream of βgal-expressing cells that emanate from the RL and travel into the subpial stream (white arrows in Figure 3). In the E14.5 *Wls*-reporter cerebellum, Msx1 and βgal continue to co-express in the iRL (yellow arrows in Figure 3), while βgal still marks the cells that migrate out of the RL into the EGL; Msx1 is absent from the eRL and EGL (Figure 3).

Previously, Duval et al. (2014) have shown through lineage tracing analysis of Msx1 and Msx2 in the murine dorsal spinal cord that almost all Atoh1-positive cells at E10.5 arise from progenitors expressing Msx1 as early as E9.25 (Duval et al., 2014). In the cerebellar RL, Msx1 is expressed in the same compartments as Wls, and Wls-expressing cells are the progenitor population that give rise to the Atoh1-positive cells that are committed to glutamatergic lineages. This expression pattern of Msx1 point to a possibility that expression of Msx1 precedes that of Atoh1 in the cerebellum RL. To investigate the relationship of Msx1, as well as Msx2, with Atoh1, we examined their expression in the *Atoh1*-null cerebellum. In the E12.5 *Atoh1*-null cerebellum, *Msx1* expression in the RL persisted (Figure 4). Moreover, *Msx1* expression is no longer restricted to the distal tip of the RL and expands to a larger domain in *Atoh1*-null RL (Figure 4). *Msx2* expression is also found to persist in the *Atoh1*-null cerebellum, and its expression pattern is similar to that in the control cerebellum (Figure 4). *Msx1* expression in the *Atoh1*-null RL is found to overlap with that of *Msx2*, in contrast to their non-overlapping expression in the wildtype cerebellum. While expression of *Msx1* and *Msx2* persisted in *Atoh1*-null cerebellum, the *Msx1-Msx2-Msx1* banding pattern we previously observed in the wildtype RL is absent.

Similar to our current results of Msx1 and Msx2 expressions preceding Atoh1 in the cerebellum, it is known from our previous work that Wls in the cerebellum precedes Atoh1 expression (Yeung et al., 2014). To determine the relationship between Msx1 and Wls, we examined *Msx1* expression in the *Wls* knockout cerebellum. Figure 5 illustrates that in the E12.5 *Wls* knockout cerebellum, *Msx1* expression is still observed in the RL, suggesting that Msx1 expression in the cerebellum is independent of Wls.

Msx3-positive cells mark the boundary region in the neuroepithelium between the Atoh1 and Ptf1a domains at E12.5

As seen with chromogenic ISH analysis, *Msx3* is expressed throughout the VZ at E11.5 and E12.5 (Black arrows in Figures 1E,H). To determine if *Msx3* expression extends to the RL, double-labeling FISH for *Msx3* and the RL marker *Atoh1* was examined at E12.5 (Figure 6). This revealed that *Msx3* expressing cells do not overlap with *Atoh1* expressing cells and a boundary can be observed between their respective domains (Figures 6A–C). FISH double label with *Msx3* and *Ptf1a* at E12.5 revealed that they largely overlap in their expression domains in the VZ, with a notable exception that the posterior-most expression boundaries, near the RL, do not coincide (Figures 6D–F). This is also observed at E11.5 (Figures 6G–I). *Msx3* expression extends more posteriorly compared to *Ptf1a* expression at E11.5 and E12.5 (the region between the white arrows in Figures 6D,G). Thus, *Msx3* expression at its posterior edge creates a molecular demarcation between the non-overlapping *Atoh1* and *Ptf1a* expressing regions (Figures 6J–L). To test if the posterior-edge expression of *Msx3* is restricted by the expression of *Atoh1*, we examined *Msx3* expression in the absence of *Atoh1*. In the E12.5 *Atoh1*-null cerebellum, cells expressing Msx3 were found to be sharing a boundary with Msx1 expressing cells, in sharp contrast to the wildtype cerebellum in which the two expression domains are separated by a gap (Figure 7). Despite the changes in expression domain of *Msx1*+ and *Msx3*+ cells, no cells are found to co-express both genes in the E12.5 *Atoh1*-null cerebellum (Figures 7A,C–F).

Msx3-positive cells are restricted to the posterior region of the proliferative ventricular zone at E14.5 in the lateral cerebellum

While *Msx3* is expressed throughout the VZ at E11.5 and E12.5, *Msx3* expression becomes restricted within the VZ at later time-points. The spatial dynamics of *Msx3* expression along the medio-lateral axis at E12.5 noted earlier becomes more obvious at E14.5 (Figure 8). In the most lateral aspect of the cerebellum, *Msx3* occupies

10.3389/fnmol.2024.1356544

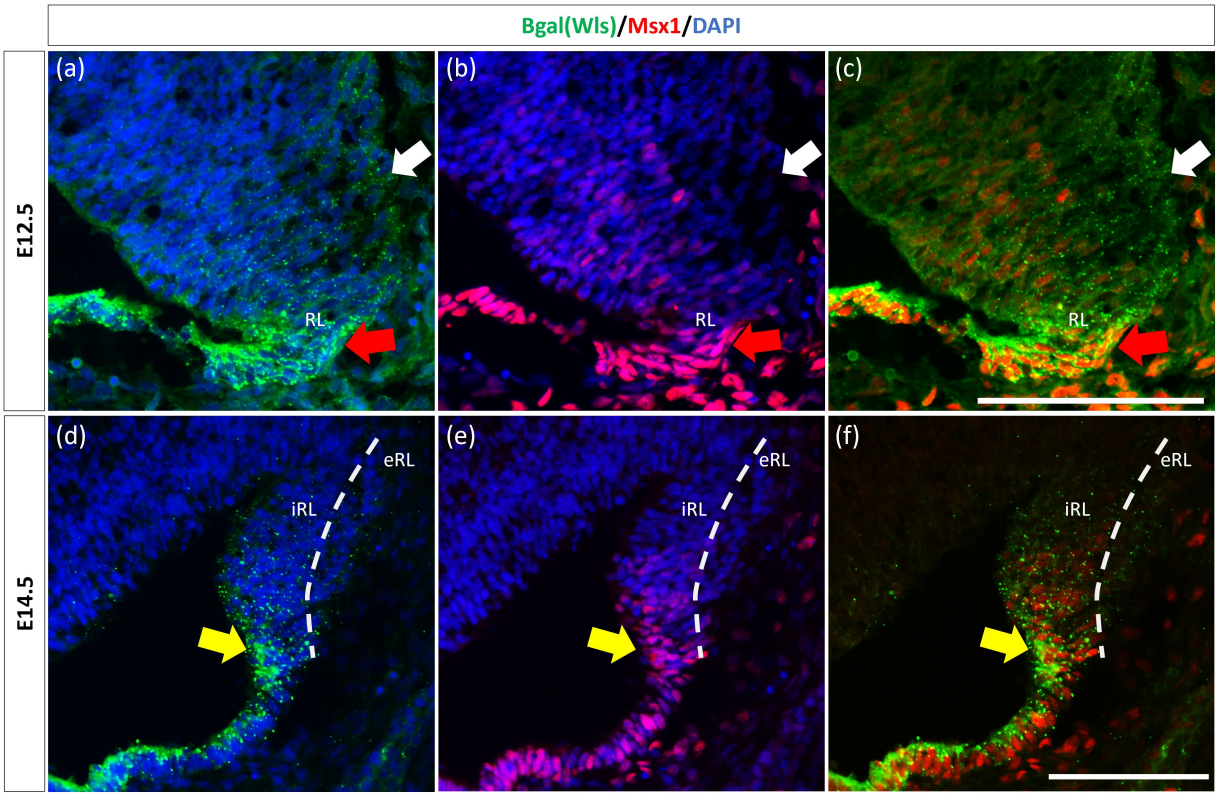

FIGURE 3
Msx1 and Wls expression in the developing cerebellar rhombic lip. Expression of Wls and Msx1 was examined in Wls-βgal reporter mouse embryos at E12.5 **(A–C)** and E14.5 **(D–F)**. At E12.5, Msx1 and Wls are co-expressed strongly in the distal tip of the RL (red arrows), co-expression of both molecules can also be seen in the RL area. Msx1, however, is not expressed in the Wls-positive subpial stream (white arrows) populated by the RL-lineage progenitors emanating from the RL. At E14.5, Msx1 and Wls continue to co-express and localize to the iRL (yellow arrows) while Msx1 expression is absent in the eRL. eRL, exterior face of the RL; RL, Rhombic Lip; iRL, interior face of the RL. Scale bars, 100 μm.

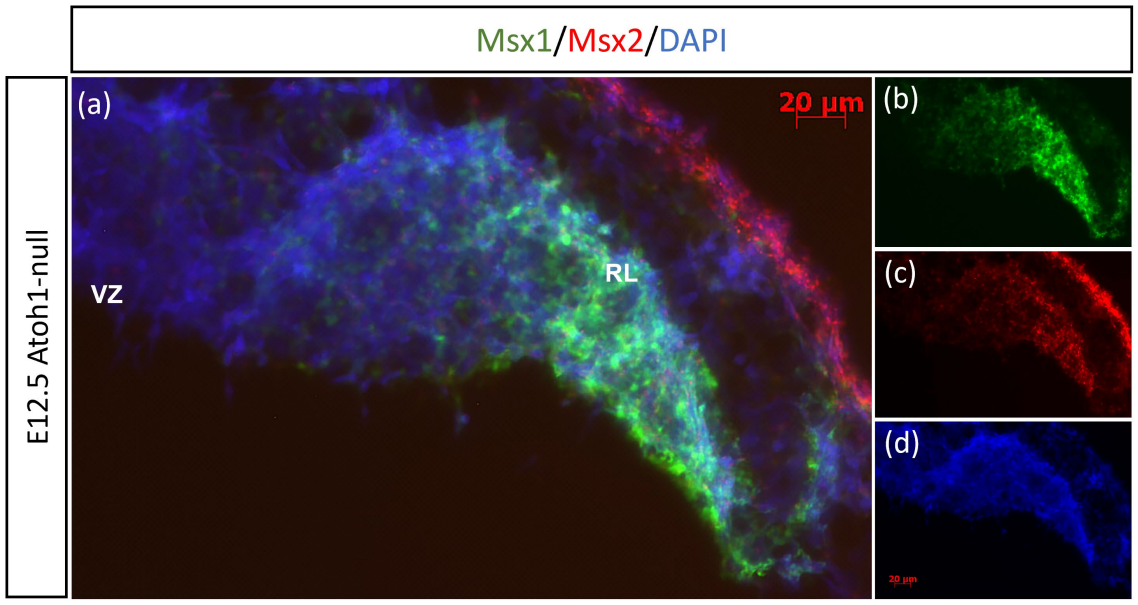

FIGURE 4
Msx1 and Msx2 expression in E12.5 Atoh1-null cerebellum. **(A–D)** The FISH double-labeling of Msx1 and Msx2 in the E12.5 *Atoh1*-null cerebellum indicates their expression persistence **(A)**. While the expression pattern of Msx1 expands to a larger domain in *Atoh1*-null RL **(B)**, Msx2 expression is similar to that in the control cerebellum **(C)**. **(D)** is DAPI (blue) as counterstain. RL, Rhombic Lip; VZ, ventricular zone. Scale bars, 20 μm.

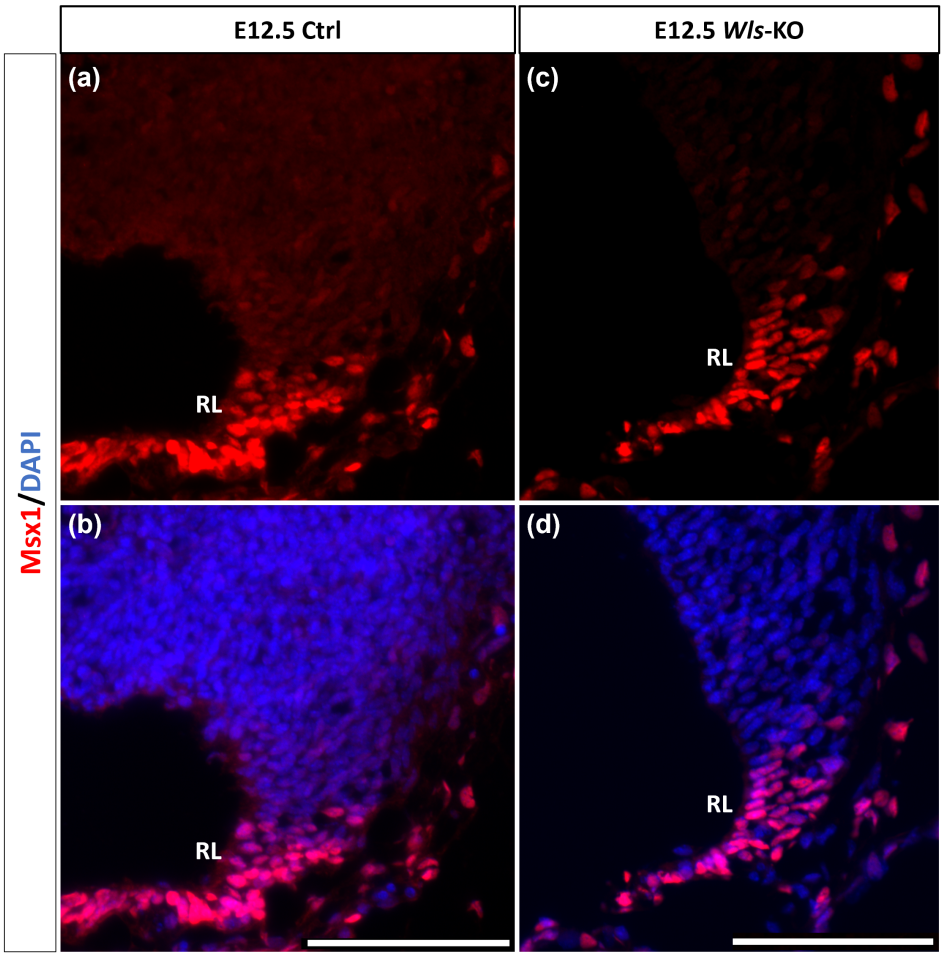

FIGURE 5
Msx1 expression in E12.5 *Wls*-knockout mutant and control cerebella. In control cerebellum **(A,B)**, Msx1 is expressed in the RL. Expression of Msx1 in the RL is persisted in the *Wls* knockout cerebellum **(C,D)** and similar to Msx1 expression in the control RL. RL, rhombic lip. Scale bars, 100 μm.

a small region in the posterior part of the VZ near the RL (Figures 8A,B) and progressively occupies the entire VZ at the most medial aspect of the cerebellum (Figures 8E,F).

We examined cell proliferation in the VZ within the *Msx3* expressing domain using FISH along with BrdU immunohistochemistry. We used BrdU labeling to mark cells that are proliferating 1 h before we harvest the embryos at E14.5 (Figure 9). *Msx3* expression along the medio-lateral axis was found to be strictly within the proliferative region of the neuroepithelium.

Discussion

The members of the *Msx* gene family are homeobox-containing, highly conserved transcription factors, previously unexplored in the context of the cerebellum. *Msx* genes are known best as downstream effector molecules of BMP signaling, which is a crucial signaling pathway for the cerebellum via the roof plate epithelial cells posteriorly adjacent to the developing cerebellar primordium (Krizhanovsky and Ben-Arie, 2006). In our examination, the *Msx* genes are found to pattern the proliferative neuroepithelium of the early embryonic cerebellar primordium. High resolution RNAscope reveals that *Msx1* marks the *Atoh1*-negative distal tip of the RL, while *Msx2* does not overlap with *Msx1* and marks the *Atoh1*-positive rhombic lip; *Msx3* is expressed in the *Ptf1a*-positive ventricular zone but also demarcates a *Ptf1a*-negative region that neighbors the rhombic lip. This spatial patterning brings new dimensions to our understanding of compartmentation of the cerebellar neuroepithelium and is summarized in Figure 10A.

We find that all 3 *Msx* genes persist in the *Atoh1*-null cerebellum, placing them as BMP signaling effector molecules preceding (*Msx1* and *Msx2*), or independent (*Msx3*), of *Atoh1*. Upon *Atoh1* ablation, *Msx1* and *Msx3* expressions in the cerebellar germinal zones shift. These findings indicate that *Atoh1* inhibits the expression of *Msx1* and *Msx3* in the normal developing cerebellum, and place the *Msx* genes in a dynamic regulatory network with *Atoh1* (see Figure 10B for summary schematic). As external signaling molecules, the BMPs have been implicated in the specification of cerebellar cell types but their downstream molecular cascades are unknown. The results of this study present the *Msx* genes as strong candidates facilitating this BMP signaling in cerebellum development.

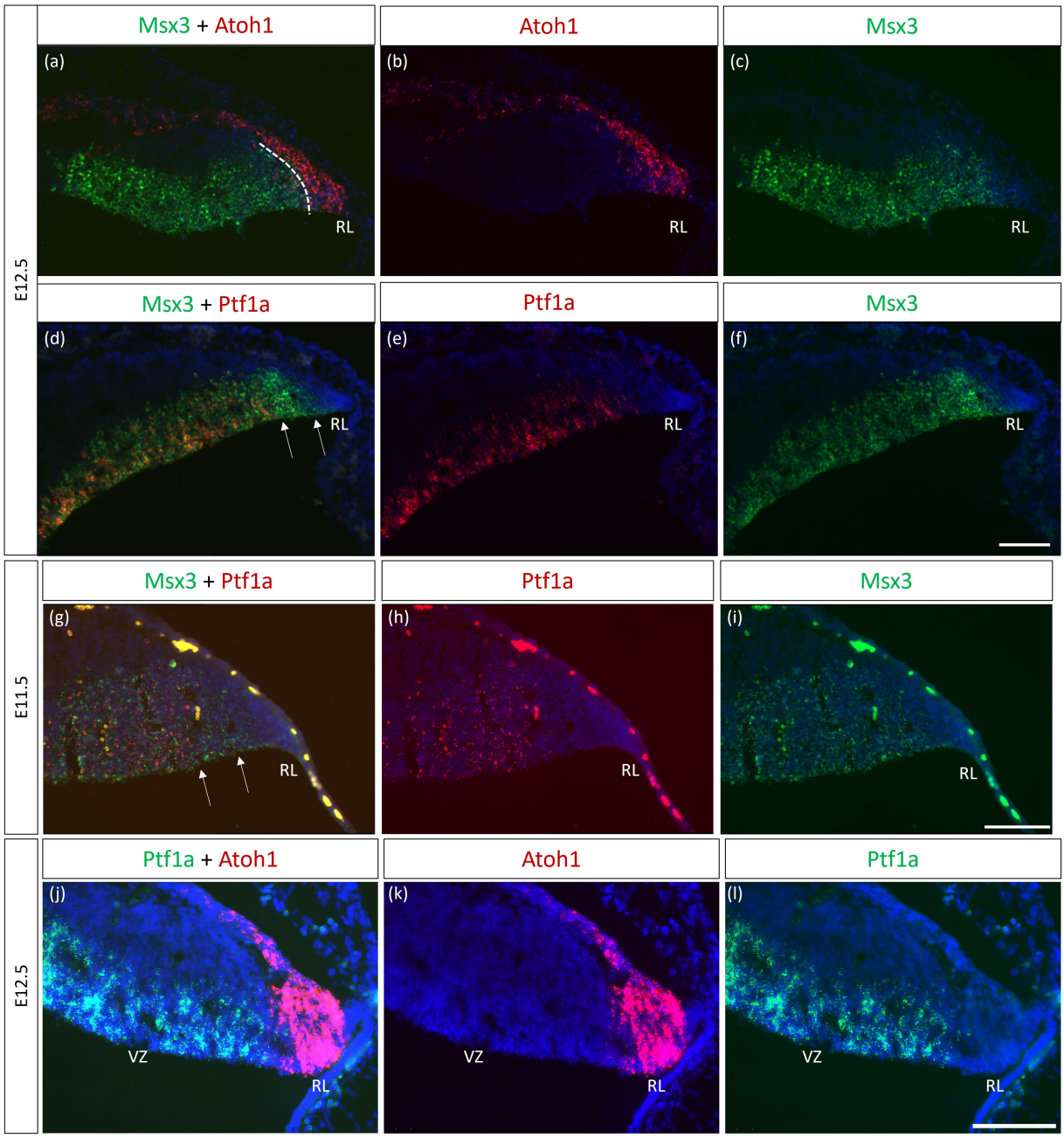

FIGURE 6
Msx3 expression relative to Atoh1 and Ptf1a in the early cerebellum. **(A–F, J–L)** RNAscope FISH double-label on E12.5 cerebellum. **(A–C)** Co-labeling of Msx3 (green) and Atoh1 (red) illustrates that Msx3 and Atoh1 do not overlap; this boundary is marked by the dashed line. **(D–F)** Co-labeling of Msx3 (green) and Ptf1a (red) illustrates a large overlap in their regions of expression in the VZ. The Msx3 boundary extends further than the Ptf1a boundary and abuts the RL (arrows). **(G–I)** RNAscope double-label on sagittal E11.5 sections with Msx3 (green) and Ptf1a (red) shows the same Msx3-exclusive region near the RL (arrows). **(J–L)** The co-staining of Ptf1a (green) and Atoh1 (red) in the E12.5 wild type cerebellum indicates their expression in the VZ and RL, respectively, with no overlap. Note that the roof plate epithelium has auto-fluorescence giving rise to the blob-like artifacts (refer to Supplementary Figure 5A for negative control staining). For orientation purposes, sagittal sections are shown with the right side of the panels denoting dorsal and bottom side denoting ventral. All panels have DAPI (blue) as counterstain. RL, Rhombic Lip. Scale bars, 100 μm.

Msx3 as a key regulator of the ventricular zone

Msx3 is the most understudied member of the family. *Msx3* is yet to be confirmed as a direct transcriptional target of BMP signaling, although ectopic BMP expression can induce *Msx3* (Shimeld et al., 1996). Unlike the other family members, *Msx3* is present exclusively in the dorsal murine CNS tissue (Sunkin et al., 2013). Our characterization of *Msx3* at E12.5 with known germinal zone markers, Ptf1a and Atoh1, revealed an intriguing pattern along the VZ and RL at this time of early cerebellar development. The current view of the cerebellar neuroepithelia depicts the VZ as marked by Ptf1a + cells throughout. In our present findings, however, *Msx3* is expressed in the VZ and forms a boundary with the *Atoh1*+ cells in the RL. While

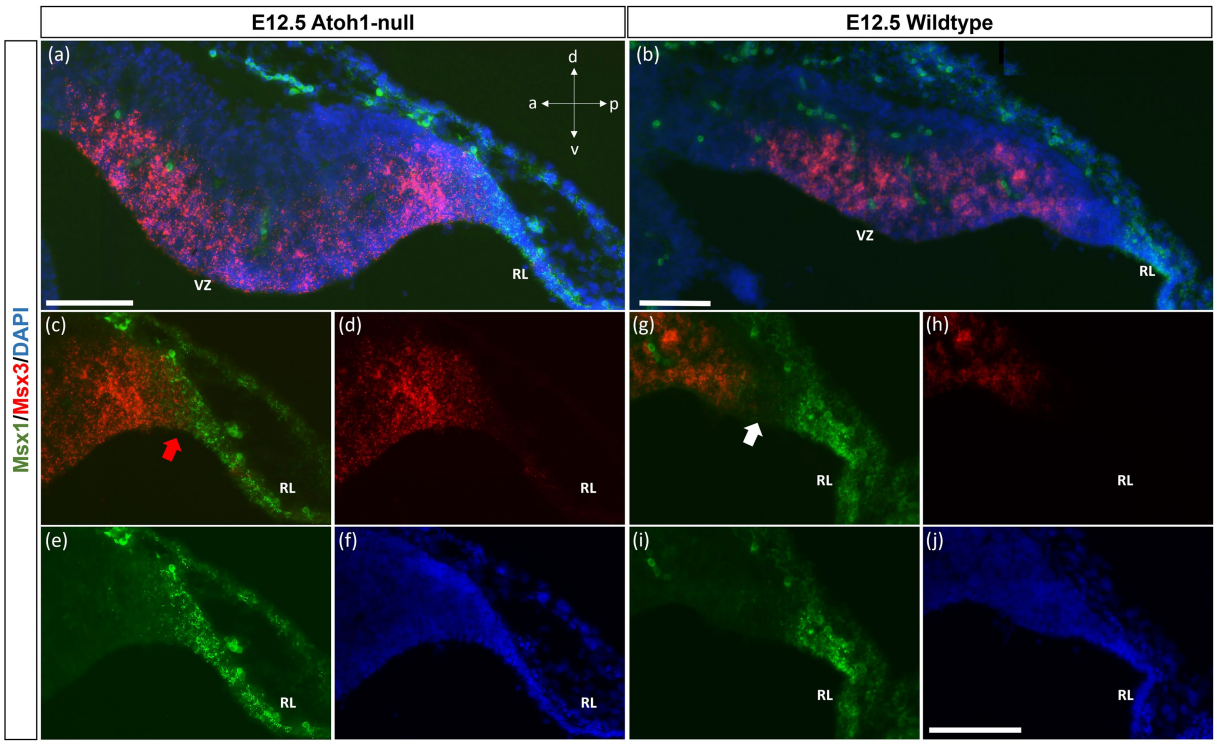

FIGURE 7
Msx1 and Msx3 expression in E12.5 Atoh1-null and wildtype cerebella. **(A,B)** The FISH double-labeling of Msx1 and Msx3 in the E12.5 *Atoh1*-null (a,a') and wildtype cerebella (b,b'). (a' and b') illustrate that the sections from mutant and wildtype are collected at the same medio-lateral position. **(C–F)** Expression of Msx1 and Msx3 shifts and now sharing a boundary in the *Atoh1*-null cerebellum as denoted by the red arrow in **(C)**. Panels **(A,C–F)** indicate Msx1 and Msx3 expression persistence in the *Atoh1*-null cerebellum. The shift of Msx1 and Msx3 expression, however, does not result in cells that co-express Msx1 and Msx3 **(A,C–E)**. **(G–I)** A very different picture is shown in the wildtype cerebellum where there is a notable gap between cells that express Msx3 and Msx1 as noted by white arrow in **(G)**. **(F,J)** DAPI (blue) used as a counterstain. RL, Rhombic Lip; VZ, ventricular zone. All scale bars, 100 μm.

Msx3 largely overlaps with *Ptf1a* in the VZ, Msx3 expression extends beyond the posterior end of Ptf1a-positive zone, as shown by a gap between *Ptf1a*-positive VZ and *Atoh1*-positive RL; and here there is an *Msx3*-exclusive region. The *Msx3*-exclusive region, defined as *Atoh1*-negative/*Ptf1a*-negative/*Msx3*-positive, has not been previously identified and invites the question of what cells arise from it.

In a recent single-cell RNA sequencing of the early cerebellum, a rare group of cells with mixed features of RL and VZ (i.e., expressing both *Atoh1* and *Ascl1*) have been identified suggesting that parts of the RL and VZ lineages may have a common origin (Khouri-Farah et al., 2022). Zhang et al. (2021) report a common progenitor that generates glutamatergic and GABAergic lineages, and detected a similar rare cell group (Atoh1- and Ptf1a-positive) at the border of RL and VZ (Zhang et al., 2021). This seems to overlap with the *Msx3*-exclusive region we identify in the present study. Further research that examines the lineage tracing of *Msx3*-expressing cells (possible bipotent progenitors) in comparison to that of *Ptf1a*-expressing cells (GABAergic lineage) will address whether *Msx3* demarcates a population of bipotential progenitors in the VZ of cerebellar primordia.

The *Msx3* expressing domain at E14.5 becomes more restricted to the posterior-most part of the ventricular zone, which would be exclusively the *Atoh1*-negative/*Ptf1a*-negative/*Msx3*-positive region as described before. This receding expression pattern in the ventricular zone is also shown by Olig2, a transcription factor that specifies the Purkinje cell progenitors, as well as the canonical BMP and p-SMAD1/5 molecules that form a morphogenetic gradient (Seto et al., 2014; Ma et al., 2020). Another transcription factor crucial to this zone is Gsx1 that specifies the interneuron progenitors (Seto et al., 2014). As Purkinje cells are born first from the ventricular zone, followed by interneurons, the progenitor cells of this zone express first Olig2 and then Gsx1 (Seto et al., 2014). Recently, Ma et al. (2020) have shown that the BMP and p-SMAD1/5 gradient directs the Olig2-Gsx1 based progenitor fate transition in the cerebellar ventricular zone by suppressing Gsx1 expression in the Olig2 domain of the posterior VZ (Ma et al., 2020). If Msx3 works downstream of BMP signaling to maintain the Olig2 domain, an interesting question is whether Msx3 can suppress interneuron fate or enable Purkinje cell fate, or both? In the study by Liu et al. (2004), a decrease in Pax2 positive interneurons was observed upon Msx3 overexpression in the chick dorsal neural tube (Liu et al., 2004). Additionally, in the postnatal mouse cerebellum, *Msx3* expression can be detected in the Purkinje cells but not in the interneurons (Supplementary Figure S7). A key question is whether Msx3 plays a similar role in specifying the cell populations coming from the cerebellar ventricular zone in an anterior–posterior specific pattern.

Msx1 and 2 as key regulators of the rhombic lip

Msx1 and *Msx2* are direct transcriptional targets of BMP signaling. Research on the roles of Msx1 and Msx2 in limb and tooth organogenesis points to an association between Msx genes and the

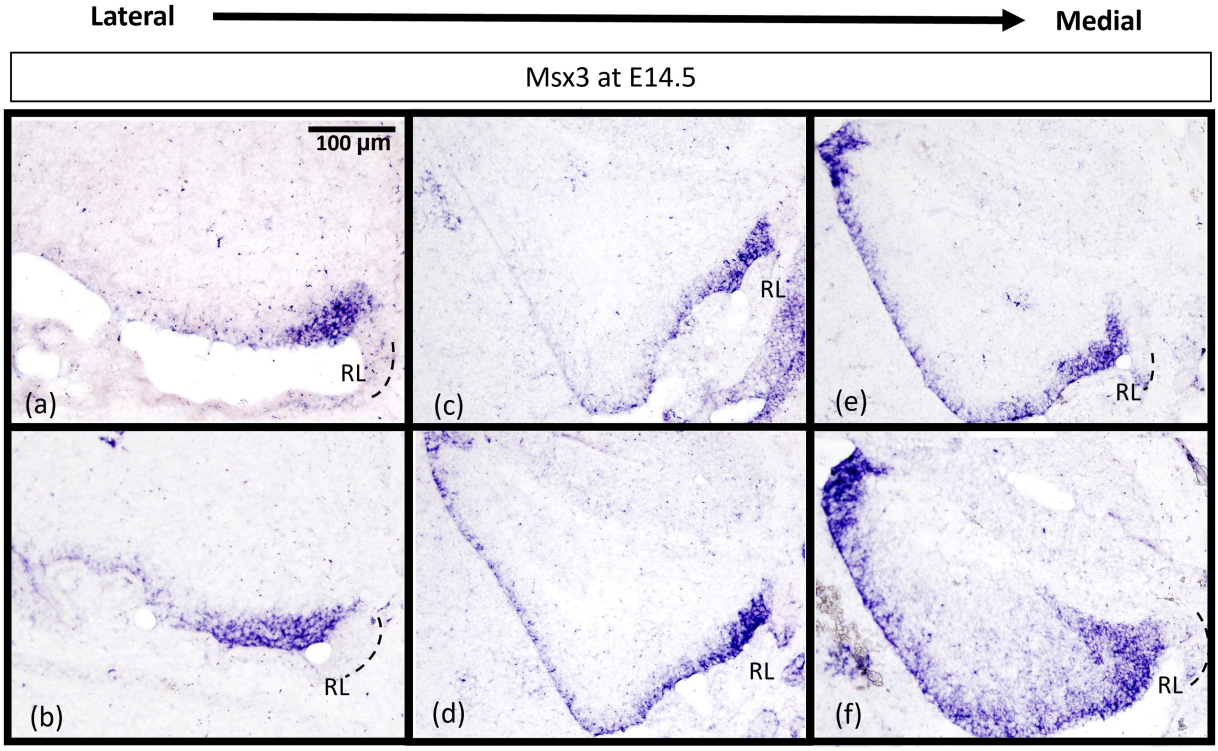

FIGURE 8
Msx3 expression is spatially dynamic within the VZ at E14.5. **(A–F)** are sagittal sections of wildtype cerebellum at E14.5, with the right side of the panels denoting posterior and bottom side denoting ventral. RNA *in situ* hybridization of Msx3 in increasing order of relative medio-lateral positions with **(A)** being the most lateral, **(B)** being more medial than **(A)**, and so on with **(F)** being the most medial. Msx3 gets restricted to the posterior end of the lateral VZ **(A,B)** and progressively occupies the entire VZ in the medial sections **(E,F)**. Refer to Appendix Figure 2C for negative control staining. RL, Rhombic Lip. Scale bar, 100 µm.

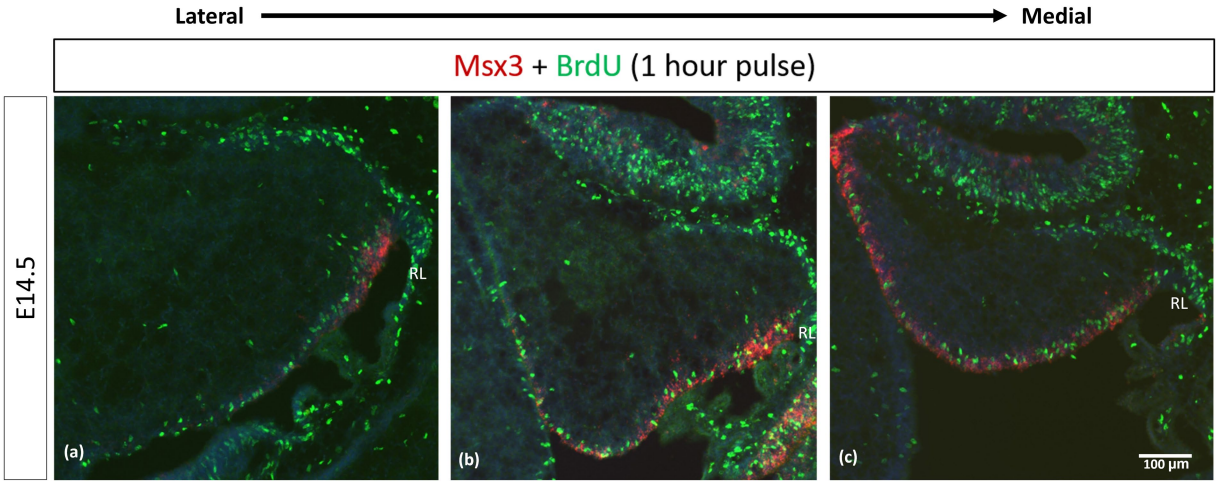

FIGURE 9
Msx3 is expressed strictly within the proliferative neuroepithelium. **(A–C)** are sagittal sections of wildtype cerebellum at E14.5, with the right side of the panels denoting posterior and bottom side denoting ventral. RNAscope FISH of Msx3 (red) with fluorescence immunohistochemistry of BrdU (green) for mouse pulsed with BrdU 1 h before E14.5 embryos were harvested. Relatively **(A)** is the most lateral and **(C)** is the most medial. RL, Rhombic Lip. Scale bar, 100 µm.

extracellular signaling control of the balance between proliferation and differentiation (Dodig et al., 1999; Liu et al., 1999; Odelberg et al., 2000; Satokata et al., 2000; Nechiporuk and Keating, 2002; Lallemand et al., 2005). Many studies suggest a possible redundancy in Msx1 and Msx2 functions in various tissue types or organ systems (Catron et al., 1996; Bei and Maas, 1998; Han et al., 2003; Lallemand et al., 2005; Han et al., 2007; Chen et al., 2008). In the context of the cerebellum, we noted that in adult stages, postmitotic granule cells express *Msx2*

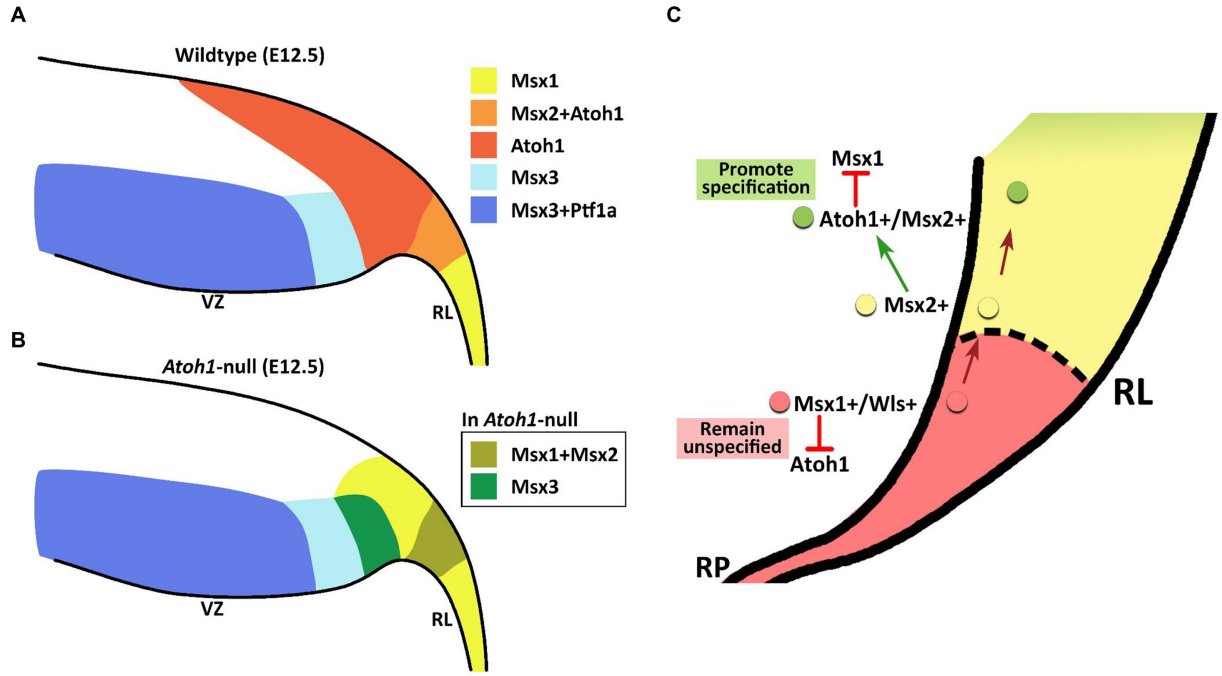

FIGURE 10
Schematic illustration of Msx expression in the early embryonic cerebellar neuroepithelium. **(A)** During early cerebellum development, expression patterns of Msx genes within the neuroepithelium demarcate the VZ and RL into molecularly distinct regions. Msx1 expression marks the distal tip of the RL that is Atoh1-negative. Msx2 is found to be co-expressed with Atoh1 in the RL. Msx3 is expressed in the VZ and largely overlapped with expression of Ptf1a, although Msx3 expression extends beyond the posterior end of the Ptf1-positive zone and abuts the Atoh1-positive RL. **(B)** In the Atoh1-null cerebellum, all three Msx genes expression persisted. The expression of Msx1 and Msx3 in the absence of Atoh1 is observed to expand into the presumptive Atoh1 region in the RL. RL, rhombic lip; VZ, ventricular zone. **(C)** Schematic summarizing the interaction between Msx1, Msx2 and Atoh1 in patterning the developing RL. Progenitors localized to the distal tip of the RL express Msx1 and Wls; Atoh1 and other pro-neural markers are likely repressed by Msx1 for a cell to maintain an unspecified state. Msx1+/Wls + cells that are committed to the RL cell fate express Msx2, which may act upstream of Atoh1 and activate Atoh1 expression. Expression of Atoh1 in these lineage-committed cells, in turn, downregulates Msx1 which is required to promote lineage specification.

but not *Msx1* (Supplementary Figure S6). Our high-resolution expression analysis across early embryonic time and space reveals that *Msx1* and *Msx2* are expressed in the rhombic lip, albeit in different regions. *Msx2* is largely overlapping with *Atoh1*, while *Msx1* has the strongest expression in an *Atoh1* negative region of the rhombic lip that is adjacent to the roof plate. Upon *Atoh1* ablation, we found that *Msx2* expression remains unchanged but *Msx1* expressing cells expand and overlap with the *Msx2*-expressing domain. Based on distinct expression patterns of *Msx1* and *Msx2* in early and late stages, we expect their functions to also be distinct in the cerebellum.

Seminal scRNAseq studies on the developing cerebellum identified the presence of *Msx1* in 'roof plate-like cells' pointing to a region in the rhombic lip adjacent to the roof plate (Carter et al., 2018; Wizeman et al., 2019). We have previously demonstrated that RL cells that express Wls, the main regulator of Wnt molecule secretion, likely mark the progenitor pool that gives rise to the Atoh1-expressing cells in the RL (Yeung et al., 2014; Yeung and Goldowitz, 2017). We demonstrate in the present study that Msx1 and Wls are co-expressed in cells at the distal-most tip of the RL. Given that Wls expression in the RL is independent of Atoh1, we also expected that the activation of Msx1 expression to be independent of Atoh1. Our findings that Msx1 expression persisted in *Atoh1*-null cerebellum confirm this hypothesis. We noted in the *Atoh1*-null RL, however, the former Atoh1-Msx1 boundary observed in the wildtype RL was disrupted and Msx1 is expressed in the presumingly Atoh1-positive domain (i.e., Msx2-expressing domain). This observation suggests that Atoh1 has an inhibitory effect on Msx1.

In previous work on the developing spinal cord, *Msx1* and *Msx2* were shown to be upstream of *Atoh1* in the dorsal neural tube. Duval et al.'s study of *Msx1-Msx2* double mutant mouse embryos found that the *Atoh1*-expressing dorsal neural tube progenitor cells are lost (Duval et al., 2014). They have shown through lineage tracing analysis of Msx1 in the murine dorsal spinal cord that almost all Atoh1-positive cells at E10.5 arise from progenitors expressing Msx1 as early as E9.25. Additionally, their *in-vitro* study indicated that Msx1 and Msx2 bind to the Atoh1 3′ enhancer and activate Atoh1 expression. They concluded from these findings that Msx1 and Msx2 are activators of Atoh1. A similar relationship may exist in the cerebellum. Msx2 and Atoh1 are observed to be co-expressed in the RL, and Msx2 expression is independent of Atoh1 as demonstrated in the *Atoh1*-null cerebellum, suggesting that Msx2 might be an activator of Atoh1 in the cerebellar rhombic lip.

Based on our present work and previous findings, we now propose that Msx1 and Msx2 act together with Atoh1 to pattern the developing RL. The cells in the distal tip of the RL positive for Msx1 and Wls are the progenitors that give rise to Msx2- and Atoh1-positive cells that are lineage committed. It is likely that Msx2 expression in these committed cells activates the expression of Atoh1, which in turn negatively regulates the expression of Msx1 in these cells (see Figure 10C).

Msx genes and the fate of cells in the early cerebellum

Evolution of our understanding of the progenitor cells of the cerebellum has been quite remarkable over the last 50 or so years and highlights the technical advances that have been brought to bear on the analysis of cell lineage in the most complex biological system, the brain. The use of genetically inducible fate mapping has yielded a clear picture of the neurotransmitter-based lineages of the cerebellum: where GABAergic neurons arise from the ventricular neuroepithelium and are marked by Ptf1a (Glasgow et al., 2005; Hoshino et al., 2005) whereas glutamatergic neurons arise from the rhombic lip and are marked by Atoh1 (Machold and Fishell, 2005; Wang et al., 2005).

The work in our lab has focused on the glutamatergic population that emerges from the rhombic lip. In these studies, we found that the rhombic lip is organized in an inner and outer manner where the inner region is hypothesized to be a more purely generative zone while the outer region is composed of cells whose fate is more restricted. The inner zone (iRL) is marked by cells that express Wls and do not express Atoh1 (Yeung et al., 2014). The outer zone is marked by cells that express Atoh1 with diminished expression of Wls. The current study confirms and provides additional detail to this picture, with Msx1 mapping to the inner face of the RL. The role of Msx1 as a transcriptional repressor of pro-neural and pro-differentiation markers such as Atoh1, Ascl1, Ngn1, Ngn2 and Pax7, as found in the dorsal neural tube (Liu et al., 2004), would fit this model; Msx1 repressing pro-differentiation markers in the cerebellar iRL to keep the progenitor pool in a less-specified state, in tandem with Wls. It is interesting to note that a similar organization of inner and outer regions of the RL has been found in the human RL (Haldipur et al., 2019) and the molecular heterogeneity of these regions may be the key to understanding and treating the most common form on pediatric brain tumor, the medulloblastoma (Vladoiu et al., 2019; Hendrikse et al., 2022; Smith et al., 2022).

Msx1 and Msx2 genes have been shown to be regulated by, and downstream to, WNT signaling in various contexts like embryonic stem cell maintenance (Hussein et al., 2003), craniofacial development (Medio et al., 2012), and intestinal tumor development (Horazna et al., 2019). However, a recent study in tooth morphogenesis provides evidence that Msx1 is upstream of WNT signaling, and in fact regulates it (Lee et al., 2022). In all these contexts, Msx1 and WNT molecules, together, maintain a pool of progenitor cells (Medio et al., 2012; Horazna et al., 2019; Lee et al., 2022). The question remains open, however, as to whether Msx1 regulates WNT signaling in cerebellar development. In the present study, we find that Msx1 expression is unchanged in the *Wls*-cKO cerebellar RL, suggesting that Msx1 is upstream of WNT signaling in the cerebellum.

The present study is the first to examine the patterning and potential roles of the *Msx* genes in cerebellar development. Our results place the *Msx* genes as strong candidates for facilitating BMP signaling in the cerebellum. As transcription factors that are immediate effectors of external BMP signaling from the roof plate, the *Msx* genes are likely to be upstream players of molecular cascades underlying transcriptional regulation of cell types emerging during cerebellar development, given that they play similar roles in limb, tooth, and spinal cord development (Bei and Maas, 1998; Liu et al., 2004; Lallemand et al., 2005; Han et al., 2007; Duval et al., 2014). Further studies cementing the regulation of the *Msx* genes by BMP/SMAD signaling in cerebellum would provide directions in this emerging picture of the earliest cell fate decisions in cerebellar development.

Based on our findings, we present the *Msx* genes as candidate novel regulators of early cerebellar progenitors that precede lineage-committed progenitors like the Atoh1-positive cells in the rhombic lip. The early expression patterns of the *Msx* genes suggest a potential function in progenitor cell maintenance and specification, and present as strong candidates for facilitating BMP signaling in cerebellum development.

Methods

Animal husbandry

The *Wls*-reporter ($Wls^{LacZ/+}$) mouse strain was bred and genotyped according to the protocol previously described (Yeung et al., 2014). The *Wls* knockout embryos were generated, phenotype and genotyped according to the protocol previously described (Yeung and Goldowitz, 2017). To harvest tissues at embryonic time points, timed pregnancies were set up. The morning a vaginal plug was detected was designated as embryonic day 0.5 (E0.5). All animal procedures are conducted in accordance with the guidelines of the Animal Care Committee (ACC) at University of British Columbia.

Atoh1-null embryos were received from Dr. Huda Zoghbi at the Baylor College of Medicine. The mice were bred, phenotyped and genotyped by the Zoghbi lab according to the protocol previously described (Wang et al., 2005). The animal procedures related to *Atoh1*-null samples are carried out in accordance with The Baylor College of Medicine Institutional Animal Care and Use Committee.

Tissue preparation and histology

Embryos harvested between E10.5 and E15.5 were immersion-fixed in 4% paraformaldehyde made in 0.1 M PB (phosphate buffer) for 1 h on ice. Embryos harvested at E16.5 and onwards were first trans-cardially perfused with 0.1 M PBS (phosphate-buffered saline) and then followed by 4% paraformaldehyde in 0.1 M PB, brains were dissected out, and then immersion-fixed in 4% paraformaldehyde in 0.1 M PB for 1 h on ice. Fixed tissues were rinsed thrice with 0.1 M PBS followed by cryoprotection in 30% sucrose solution in 0.1 M PBS overnight at 4°C before embedding them in optimal cutting temperature (OCT) compound (Tissue-Tek #4583). Tissue was cryosectioned in sagittal orientation at −20°C at 12 µm thickness, mounted on Superfrost slides (Fisher Scientific #12–550-15), air dried at room temperature and stored at −80°C until use. For all histological experiments, at least 3 different embryos were used with multiple sections per embryo.

RNA *in situ* hybridization

Digoxigenin-UTP labeled riboprobes (antisense and sense) were generated corresponding to the cDNA of Msx1, Msx2, and Msx3. The cDNA was amplified from a cDNA library made from E12.5 mouse cerebellum using Invitrogen SuperScript IV First-Strand Synthesis System (Invitrogen #18091050). The following primers were used:

Gene Name	Forward Primer 5′-3’	Reverse Primer 5′-3’	Riboprobe Position (NCBI Reference)
Msx1	CCGAAAGCCCCGAGAAACTA	GCTGGGGACCACGGATAAAT	653–1,470 (NM_010835.2)
Msx2	GCGGTGACTTGTTTTCGTCG	TTTGTGAGAGGAAAGGGGGC	90–1,095 (NM_013601.2)
Msx3	CCCTCCGCAAACACAAAACC	CTTCCAAGTCCATCCAGCGT	396–1,344 (NM_001347609.1)

This cDNA was cloned into pGEM-T Easy vector (Promega #A1360) and a combination of gene-specific primers and M13 primers were used to generate DNA templates which were then reverse transcribed using T7 and SP6 polymerases to generate the cRNA probes. The probes were denatured for 10 min at 72°C before being added to the hybridization buffer (Ambion, Invitrogen #AM8670). The tissue sections were acetylated with acetic anhydride in 0.1 M triethanolamine and dehydrated with increasing concentrations of ethanol before hybridizing them with the probes overnight at 68°C in a humid chamber. Then, they were washed in saline sodium citrate (SSC) solutions: 4xSSC, 2xSSC, 1xSSC and 0.5xSSC at 55°C followed by anti-Digoxigenin antibody (Roche #11093274910, 1:500) incubation for 2 h at room temperature. After washes, sections were colorized with NBT/BCIP (Roche #11681451001), fixed in 4% PFA, dehydrated and cleared in graded ethanol solutions and Xylene, and coverslipped with Permount diluted in Xylene.

Rnascope® fluorescence *in situ* hybridization

To look at RNA level expression of 2 genes simultaneously, and at higher resolution, Bio-techne ACD's RNAscope Multiplex Fluorescent V2 Assay kit (single molecule RNA fluorescent *in situ* hybridization) was used according to manufacturer's instructions. The RNAscope technology uses tyramide signal amplification which suppresses background and boosts the signal such that individual RNA molecules can be detected as single dot punctae - The "ZZ" probe design only allows amplification to build upon consecutively bound probes on the target, thereby ensuring that each punctate dot represents only real signal (Wang et al., 2012, 2013). Briefly, the slides were post-fixed in 4% PFA for 30 min, dehydrated in graded ethanol solutions and permeabilized with a protease treatment for 15–30 min depending on the tissue age. Slides were then hybridized with the probes overnight at 40°C. After this, the signal amplification tree was built by sequentially incubating slides in Amplifiers 1,2 and 3 at 40°C. The first amplification strand, Amplifier 1, only hybridizes to the "ZZ" s. This was followed by developing the fluorescent channels that involved incubation with HRP attached to the channel-specific sequence, adding the fluorescent dye, and then adding HRP blockers so the other channels can be developed similarly. All these incubations were done at 40°C for durations based on the user manual guide provided by the manufacturer. After the final HRP blocking step, slides were incubated in DAPI to counterstain for 5 min before coverslipping with FluorSave mounting medium (Millipore #345789). RNAscope protocol dictates a short DAPI treatment to ensure that the punctate dots (real signal) are visible and not visually overpowered by the much larger nuclear DAPI staining.

Immunofluorescence

Tissue sections mounted on slides were warmed on slide warmer at 37°C. Then the sections were rehydrated in 0.1 M PBS, followed by incubation in 0.1 M PBS-T (0.1% Triton X-100 in 0.1 M PBS) for permeabilization. Sections were incubated in a blocking solution (1% BSA and 10% normal serum in 0.1 M PBS-T) at room temperature for 30 min in a humidified chamber. Subsequently, the blocking solution will be replaced by a diluted primary antibody (see table) in the incubation solution (1% BSA and 5% normal serum in 0.1 M PBS-T) and incubated at 4°C overnight in a humidified chamber. The sections were washed 3 times in 0.1PBS-T the next day. The sections were then incubated in secondary antibodies diluted in the incubation solution and counterstained using DAPI. The sections were washed 3 times in 0.1 M PB and 1 time in 0.01 M PB. Coverslip was applied on the slides with mounting media FluorSave.

BrdU labeling

To look at proliferative cells in the cerebellar ventricular zone, pregnant female mouse with E14.5 embryos was intraperitoneally injected with 5-bromo-deoxyuridine (BrdU, Sigma #B5002; 50 µg/g body weight) 1 h before collecting the embryos. The pulse duration was 1 h because the cells are rapidly dividing at this age. Tissue sections were prepared as described above. Tissue sections underwent a 1 M HCl incubation at 37°C for 30 min post rehydration in 0.1 M PBS. The sections were incubated with the Rat anti BrdU primary antibody (1:500, AbCam #AB6326).

Microscopy

Images were taken using a Zeiss Axiovert 200 M microscope with the Axiocam/Axiovision software (Carl Zeiss).

Antibody	Concentration (Immunofluorescence)	Source and identifier
Rabbit anti-Atoh1	1:500	Proteintech 21,215-1-AP
Rabbit anti-β-galactosidase	1:500	Invitrogen A11132
Rat anti-BrdU	1:500	AbCam AB6326
Rabbit anti-Lmx1	1:2000	Millipore AB10533
Goat anti-Msx1	1:50	Rndsystems AF5045
Alexa Fluor 594 Chicken anti-Goat IgG (H + L)	1:1000	Invitrogen A-21468
Alexa Fluor 488 Chicken anti-Rabbit IgG (H + L)	1:1000	Invitrogen A-21441
Alexa Fluor 488 Goat anti-Rat IgG (H + L)	1:1000	Jackson ImmunoResearch AB_2338351

Data availability statement

The original contributions presented in the study are included in the article/Supplementary material, further inquiries can be directed to the corresponding author/s.

Ethics statement

The animal study was approved by UBC Animal Care and Use Committee. The study was conducted in accordance with the local legislation and institutional requirements.

Author contributions

IG: Conceptualization, Formal analysis, Investigation, Methodology, Supervision, Visualization, Writing – original draft, Writing – review & editing. JY: Conceptualization, Investigation, Methodology, Visualization, Writing – original draft, Writing – review & editing. MR-B: Investigation, Methodology, Visualization, Writing – original draft, Writing – review & editing. S-RW: Resources, Writing – review & editing. DG: Conceptualization, Funding acquisition, Supervision, Writing – original draft, Writing – review & editing.

Funding

The author(s) declare that financial support was received for the research, authorship, and/or publication of this article. The support for trainees was provided by UBC Academic Award (MSc) – Cordula and Gunter Paetzold Fellowship (Ishita Gupta), Michael Smith Health Research BC Trainee Award and BC Children's Hospital Research Institute Mining for Miracles Postdoctoral Fellowship (Maryam Rahimi-Balaei). This work was supported by the Natural Sciences and Engineering Research Council (NSERC) of Canada, the BCCHRI Brain, Behavior and Development Theme, and the Howard Hughes Medical Institute (HHMI).

Acknowledgments

The authors are grateful to RIKEN FANTOM 5 Consortium for the mammoth technical and informatic efforts applied to the successful time course project and to Huda Zoghbi for the providing of *Atoh1* knockout and control embryos for analysis.

Conflict of interest

The authors declare that the research was conducted in the absence of any commercial or financial relationships that could be construed as a potential conflict of interest.

The author(s) declared that they were an editorial board member of Frontiers, at the time of submission. This had no impact on the peer review process and the final decision.

Publisher's note

Supplementary material

The Supplementary material for this article can be found online at: https://www.frontiersin.org/articles/10.3389/fnmol.2024.1356544/full#supplementary-material

References

Alder, J., Lee, K. J., Jessell, T. M., and Hatten, M. E. (1999). Generation of cerebellar granule neurons in vivo by transplantation of BMP-treated neural progenitor cells. *Nat. Neurosci.* 2, 535–540. doi: 10.1038/9189

Arner, E., Daub, C. O., Vitting-Seerup, K., Andersson, R., Lilje, B., Drabløs, F., et al. (2015). Transcribed enhancers lead waves of coordinated transcription in transitioning mammalian cells. *Science* 347, 1010–1014. doi: 10.1126/science.1259418

Bei, M., and Maas, R. L. (1998). FGFs and BMP4 induce both Msx1-independent and Msx1-dependent signaling pathways in early tooth development. *Development* 125, 4325–4333. doi: 10.1242/dev.125.21.4325

Carter, R. A., Bihannic, L., Rosencrance, C., Hadley, J. L., Tong, Y., Phoenix, T. N., et al. (2018). A single-cell transcriptional atlas of the developing murine cerebellum. *Curr. Biol.* 28, 2910–2920.e2. doi: 10.1016/j.cub.2018.07.062

Casoni, F., Croci, L., Vincenti, F., Podini, P., Riba, M., Massimino, L., et al. (2020). ZFP423 regulates early patterning and multiciliogenesis in the hindbrain choroid plexus. *Development* 147:dev190173. doi: 10.1242/dev.190173

Catron, K. M., Wang, H., Hu, G., Shen, M. M., and Abate-Shen, C. (1996). Comparison of MSX-1 and MSX-2 suggests a molecular basis for functional redundancy. *Mech. Dev.* 55, 185–199. doi: 10.1016/0925-4773(96)00503-5

Catron, K. M., Zhang, H., Marshall, S. C., Inostroza, J. A., Wilson, J. M., and Abate, C. (1995). Transcriptional repression by Msx-1 does not require homeodomain DNA-binding sites. *Mol. Cell. Biol.* 15, 861–871. doi: 10.1128/mcb.15.2.861

Chen, Y.-H., Chen, Y.-H., Ishii, M., Sucov, H. M., and Maxson, R. E. (2008). Msx1 and Msx2 are required for endothelial-mesenchymal transformation of the atrioventricular cushions and patterning of the atrioventricular myocardium. *BMC Dev. Biol.* 8:75. doi: 10.1186/1471-213x-8-75

Dodig, M., Tadic, T., Tadić, T., Kronenberg, M. S., Dacic, S., Liu, Y.-H., et al. (1999). Ectopic Msx2 overexpression inhibits and Msx2 antisense stimulates calvarial osteoblast differentiation. *Dev. Biol.* 209, 298–307. doi: 10.1006/dbio.1999.9258

Duval, N., Daubas, P., Bourcier de Carbon, C., St Cloment, C., Tinevez, J.-Y., Lopes, M., et al. (2014). Msx1 and Msx2 act as essential activators of Atoh1 expression in the murine spinal cord. *Development* 141, 1726–1736. doi: 10.1242/dev.099002

Ekker, M., Akimenko, M. A., Allende, M. L., Smith, R., Drouin, G., Langille, R. M., et al. (1997). Relationships among msx gene structure and function in zebrafish and other vertebrates. *Mol. Biol. Evol.* 14, 1008–1022. doi: 10.1093/oxfordjournals.molbev.a025707

Fernandes, M., Antoine, M., and Hébert, J. M. (2012). SMAD4 is essential for generating subtypes of neurons during cerebellar development. *Dev. Biol.* 365, 82–90. doi: 10.1016/j.ydbio.2012.02.017

Foerst-Potts, L., and Sadler, T. W. (1997). Disruption of Msx1 and Msx2 reveals roles for these genes in craniofacial, eye, and axial development. *Dev. Dyn.* 209, 70–84. doi: 10.1002/(SICI)1097-0177(199705)209:1<70::AID-AJA7>3.0.CO;2-U

Glasgow, S. M., Henke, R. M., Macdonald, R. J., Wright, C. V. E., and Johnson, J. E. (2005). Ptf1a determines GABAergic over glutamatergic neuronal cell fate in the spinal cord dorsal horn. *Development* 132, 5461–5469. doi: 10.1242/dev.02167

Ha, T. J., Zhang, P. G. Y., Robert, R., Yeung, J., Swanson, D. J., Mathelier, A., et al. (2019). Identification of novel cerebellar developmental transcriptional regulators with motif activity analysis. *BMC Genomics* 20:718. doi: 10.1186/S12864-019-6063-9

Haldipur, P., Aldinger, K. A., Bernardo, S., Deng, M., Timms, A. E., Overman, L. M., et al. (2019). Spatiotemporal expansion of primary progenitor zones in the developing human cerebellum. *Science* 366, 454–460. doi: 10.1126/science.aax7526

Han, J., Ishii, M., Bringas, P., Maas, R. L., Maxson, R. E., and Chai, Y. (2007). Concerted action of Msx1 and Msx2 in regulating cranial neural crest cell differentiation during frontal bone development. *Mech. Dev.* 124, 729–745. doi: 10.1016/j.mod.2007.06.006

Han, M., Yang, X., Farrington, J. E., and Muneoka, K. (2003). Digit regeneration is regulated by Msx1 and BMP4 in fetal mice. *Development* 130, 5123–5132. doi: 10.1242/dev.00710

Hendrikse, L. D., Haldipur, P., Saulnier, O., Millman, J., Sjoboen, A. H., Erickson, A., et al. (2022). Failure of human rhombic lip differentiation underlies medulloblastoma formation. *Nature* 609, 1021–1028. doi: 10.1038/s41586-022-05215-w

Horazna, M., Janeckova, L., Svec, J., Babosova, O., Hrckulak, D., Vojtechova, M., et al. (2019). Msx1 loss suppresses formation of the ectopic crypts developed in the Apc-deficient small intestinal epithelium. *Sci. Rep.* 9:1629. doi: 10.1038/s41598-018-38310-y

Hoshino, M., Nakamura, S., Mori, K., Kawauchi, T., Terao, M., Nishimura, Y. V., et al. (2005). Ptf1a, a bHLH transcriptional gene, defines GABAergic neuronal fates in cerebellum. *Neuron* 47, 201–213. doi: 10.1016/j.neuron.2005.06.007

Hussein, S. M., Duff, E. K., and Sirard, C. (2003). Smad4 and β-catenin co-activators functionally interact with lymphoid-enhancing factor to regulate graded expression of Msx2. *J. Biol. Chem.* 278, 48805–48814. doi: 10.1074/jbc.M305472200

Khouri-Farah, N., Guo, Q., Morgan, K., Shin, J., and Li, J. Y. H. (2022). Integrated single-cell transcriptomic and epigenetic study of cell state transition and lineage commitment in embryonic mouse cerebellum. *Sci. Adv.* 8:eabl9156. doi: 10.1126/sciadv.abl9156

Krizhanovsky, V., and Ben-Arie, N. (2006). A novel role for the choroid plexus in BMP-mediated inhibition of differentiation of cerebellar neural progenitors. *Mech. Dev.* 123, 67–75. doi: 10.1016/j.mod.2005.09.005

Lai, H. C., Klisch, T. J., Roberts, R., Zoghbi, H. Y., and Johnson, J. E. (2011). In vivo neuronal subtype-specific targets of Atoh1 (Math1) in dorsal spinal cord. *J. Neurosci.* 31, 10859–10871. doi: 10.1523/JNEUROSCI.0445-11.2011

Lallemand, Y., Nicola, M.-A., Nicola, M.-A., Ramos, C., Ramos, C., Bach, A., et al. (2005). Analysis of Msx1; Msx2 double mutants reveals multiple roles for Msx genes in limb development. *Development* 132, 3003–3014. doi: 10.1242/dev.01877

Lee, J. M., Qin, C., Chai, O. H., Lan, Y., Jiang, R., and Kwon, H. J. (2022). MSX1 drives tooth morphogenesis through controlling Wnt signaling activity. *J. Dent. Res.* 101, 832–839. doi: 10.1177/00220345211070583

Liu, Y., Helms, A. W., and Johnson, J. E. (2004). Distinct activities of Msx1 and Msx3 in dorsal neural tube development. *Development* 131, 1017–1028. doi: 10.1242/dev.00994

Liu, Y.-H., Tang, Z., Kundu, R. K., Kundu, R. K., Wu, L.-Y., Luo, W., et al. (1999). Msx2 gene dosage influences the number of proliferative osteogenic cells in growth centers of the developing murine skull: a possible mechanism for MSX2 -mediated Craniosynostosis in humans. *Dev. Biol.* 205, 260–274. doi: 10.1006/dbio.1998.9114

Ma, L., Swalla, B. J., Zhou, J., Dobias, S. L., Bell, J. R., Chen, J., et al. (1996). Expression of an Msx homeobox gene in ascidians: insights into the archetypal chordate expression pattern. *Dev. Dyn.* 205, 308–318. doi: 10.1002/(SICI)1097-0177(199603)205:3<308::AID-AJA10>3.0.CO;2-0

Ma, T. C., Vong, K. I., and Kwan, K. M. (2020). Spatiotemporal decline of BMP signaling activity in neural progenitors mediates fate transition and safeguards neurogenesis. *Cell Rep.* 30, 3616–3624.e4. doi: 10.1016/j.celrep.2020.02.089

Machold, R., and Fishell, G. (2005). Math1 is expressed in temporally discrete pools of cerebellar rhombic-lip neural progenitors. *Neuron* 48, 17–24. doi: 10.1016/j.neuron.2005.08.028

Medio, M., Yeh, E., Popelut, A., Babajko, S., Berdal, A., and Helms, J. (2012). Wnt/β-catenin signaling and Msx1 promote outgrowth of the maxillary prominences. *Front. Physiol.* 3:30582. doi: 10.3389/fphys.2012.00375

Nechiporuk, A., and Keating, M. T. (2002). A proliferation gradient between proximal and msxb-expressing distal blastema directs zebrafish fin regeneration. *Development* 129, 2607–2617. doi: 10.1242/dev.129.11.2607

Newberry, E. P., Latifi, T., Battaile, J. T., and Towler, D. A. (1997). Structure-function analysis of Msx2-mediated transcriptional suppression. *Biochemistry* 36, 10451–10462. doi: 10.1021/bi971008x

Odelberg, S. J., Kollhoff, A., and Keating, M. T. (2000). Dedifferentiation of mammalian Myotubes induced by msx1. *Cell* 103, 1099–1109. doi: 10.1016/s0092-8674(00)00212-9

Qin, L., Wine-Lee, L., Ahn, K., and Crenshaw, E. B. (2006). Genetic analyses demonstrate that bone morphogenetic protein signaling is required for embryonic cerebellar development. *J. Neurosci.* 26, 1896–1905. doi: 10.1523/jneurosci.3202-05.2006

Satokata, I., Ma, L., Ohshima, H., Bei, M., Ian, W., Nishizawa, K., et al. (2000). Msx2 deficiency in mice causes pleiotropic defects in bone growth and ectodermal organ formation. *Nat. Genet.* 24, 391–395. doi: 10.1038/74231

Satokata, I., and Maas, R. (1994). Msx1 deficient mice exhibit cleft palate and abnormalities of craniofacial and tooth development. *Nat. Genet.* 6, 348–356. doi: 10.1038/ng0494-348

Seto, Y., Nakatani, T., Masuyama, N., Taya, S., Kumai, M., Minaki, Y., et al. (2014). Temporal identity transition from Purkinje cell progenitors to GABAergic interneuron progenitors in the cerebellum. *Nat. Commun.* 5:3337. doi: 10.1038/ncomms4337

Sharman, A. C., Shimeld, S. M., and Holland, P. W. H. (1999). An amphioxus Msx gene expressed predominantly in the dorsal neural tube. *Dev. Genes Evol.* 209, 260–263. doi: 10.1007/s004270050251

Shimeld, S. M., McKay, I. J., and Sharpe, P. T. (1996). The murine homeobox gene Msx-3 shows highly restricted expression in the developing neural tube. *Mech. Dev.* 55, 201–210. doi: 10.1016/0925-4773(96)00505-9

Smith, K. S., Bihannic, L., Gudenas, B. L., Haldipur, P., Tao, R., Gao, Q., et al. (2022). Unified rhombic lip origins of group 3 and group 4 medulloblastoma. *Nature* 609, 1012–1020. doi: 10.1038/s41586-022-05208-9

Sunkin, S. M., Ng, L., Lau, C., Dolbeare, T., Gilbert, T. L., Thompson, C. L., et al. (2013). Allen brain atlas: an integrated spatio-temporal portal for exploring the central nervous system. *Nucleic Acids Res.* 41, D996–D1008. doi: 10.1093/nar/gks1042

Suzuki, A., Ueno, N., and Hemmati-Brivanlou, A. (1997). Xenopus msx1 mediates epidermal induction and neural inhibition by BMP4. *Development* 124, 3037–3044. doi: 10.1242/dev.124.16.3037

Takahashi, K., Nuckolls, G. H., Tanaka, O., Semba, I., Takahashi, I., Dashner, R., et al. (1998). Adenovirus-mediated ectopic expression of Msx2 in even-numbered rhombomeres induces apoptotic elimination of cranial neural crest cells in ovo. *Development* 125, 1627–1635. doi: 10.1242/dev.125.9.1627

Tang, S., Snider, P., Firulli, A. B., and Conway, S. J. (2010). Trigenic neural crest-restricted Smad7 over-expression results in congenital craniofacial and cardiovascular defects. *Dev. Biol.* 344, 233–247. doi: 10.1016/j.ydbio.2010.05.004

Tong, K. K., and Kwan, K. M. (2013). Common partner Smad-independent canonical bone morphogenetic protein signaling in the specification process of the anterior rhombic lip during cerebellum development. *Mol. Cell. Biol.* 33, 1925–1937. doi: 10.1128/MCB.01143-12

Tríbulo, C., Aybar, M. J., Nguyen, V. H., Mullins, M. C., and Mayor, R. (2003). Regulation of Msx genes by a bmp gradient is essential for neural crest specification. *Development* 130, 6441–6452. doi: 10.1242/dev.00878

Vladoiu, M. C., El-Hamamy, I., Donovan, L. K., Farooq, H., Holgado, B. L., Sundaravadanam, Y., et al. (2019). Childhood cerebellar tumours mirror conserved fetal transcriptional programs. *Nature* 572, 67–73. doi: 10.1038/s41586-019-1158-7

Wang, W., Chen, X., Xu, H., and Lufkin, T. (1996). Msx3: a novel murine homologue of the Drosophila msh homeobox gene restricted to the dorsal embryonic central nervous system. *Mech. Dev.* 58, 203–215. doi: 10.1016/S0925-4773(96)00562-X

Wang, F., Flanagan, J., Su, N., Wang, L. C., Bui, S., Nielson, A., et al. (2012). RNAscope: a novel in situ RNA analysis platform for formalin-fixed, paraffin-embedded tissues. *J. Mol. Diagn.* 14, 22–29. doi: 10.1016/j.jmoldx.2011.08.002

Wang, Z., Portier, B. P., Gruver, A. M., Bui, S., Wang, H., Su, N., et al. (2013). Automated quantitative RNA in situ hybridization for resolution of equivocal and heterogeneous ERBB2 (HER2) status in invasive breast carcinoma. *J. Mol. Diagn.* 15, 210–219. doi: 10.1016/j.jmoldx.2012.10.003

Wang, V. Y., Rose, M. F., and Zoghbi, H. Y. (2005). Math1 expression redefines the rhombic lip derivatives and reveals novel lineages within the brainstem and cerebellum. *Neuron* 48, 31–43. doi: 10.1016/j.neuron.2005.08.024

Wizeman, J. W., Guo, Q., Wilion, E. M., and Li, J. Y. H. (2019). Specification of diverse cell types during early neurogenesis of the mouse cerebellum. *eLife* 8:3888. doi: 10.7554/eLife.42388

Wu, L. Y., Li, M., Hinton, D. R., Guo, L., Jiang, S., Wang, J. T., et al. (2003). Microphthalmia resulting from Msx2-induced apoptosis in the optic vesicle. *Investig. Ophthalmol. Vis. Sci.* 44, 2404–2412. doi: 10.1167/iovs.02-0317

Yeung, J., and Goldowitz, D. (2017). Wls expression in the rhombic lip orchestrates the embryonic development of the mouse cerebellum. *Neuroscience* 354, 30–42. doi: 10.1016/J.NEUROSCIENCE.2017.04.020

Yeung, J., Ha, T. J., Swanson, D. J., Choi, K., Tong, Y., and Goldowitz, D. (2014). Wls provides a new compartmental view of the rhombic lip in mouse cerebellar development. *J. Neurosci.* 34, 12527–12537. doi: 10.1523/JNEUROSCI.1330-14.2014

Zhang, H., Catron, K. M., and Abate-Shen, C. (1996). A role for the Msx-1 homeodomain in transcriptional regulation: residues in the N-terminal arm mediate TATA binding protein interaction and transcriptional repression. *Proc. Natl. Acad. Sci. USA* 93, 1764–1769. doi: 10.1073/pnas.93.5.1764

Zhang, T., Zhang, T., Liu, T., Mora, N., Guegan, J., Bertrand, M., et al. (2021). Generation of excitatory and inhibitory neurons from common progenitors via notch signaling in the cerebellum. *Cell Rep.* 35:109208. doi: 10.1016/j.celrep.2021.109208

Zhou, Y. X., Zhao, M., Li, D., Shimazu, K., Sakata, K., Deng, C. X., et al. (2003). Cerebellar deficits and hyperactivity in mice lacking Smad4. *J. Biol. Chem.* 278, 42313–42320. doi: 10.1074/jbc.M308287200